Proceedings of the ASME 2007 International Design Engineering Technical Conferences & Computers and Information in Engineering Conference
IDETC/CIE 2007
September 4-7, 2007, Las Vegas, Nevada, USA

DETC2007-34606

FORWARD AND INVERSE DISPLACEMENT ANALYSIS OF A NOVEL THREE-LEGGED MOBILE ROBOT BASED ON THE KINEMATICS OF IN-PARALLEL MANIPULATORS

Ping Ren
RoMeLa: Robotics & Mechanisms Laboratory
Mechanical Engineering Department
Virginia Polytechnic and State University
Blacksburg, Virginia 24061
Email: renping@vt.edu

Ivette Morazzani
RoMeLa: Robotics & Mechanisms Laboratory
Mechanical Engineering Department
Virginia Polytechnic and State University
Blacksburg, Virginia 24061
Email: imorazza@vt.edu

Dennis Hong[1]
RoMeLa: Robotics & Mechanisms Laboratory
Mechanical Engineering Department
Virginia Polytechnic and State University
Blacksburg, Virginia 24061
Email: dhong@vt.edu

ABSTRACT

This paper presents the forward and inverse displacement analysis of a novel three-legged walking robot STriDER (Self-excited Tripedal Dynamic Experimental Robot). STriDER utilizes the concept of passive dynamic locomotion to walk, but when all three feet of the robot are on the ground, the kinematic structure of the robot behaves like an in-parallel manipulator. To plan and control its change of posture, the kinematics of its forward and inverse displacement must be analyzed.

First, the concept of this novel walking robot and its unique tripedal gait is discussed including strategies for changing directions, followed by the overall kinematic configuration and definitions of its coordinate frames. When all three feet of the robot are on the ground, by assuming there are no slipping at the feet, each foot contact point are treated as a spherical joint. Kinematic analysis methods for in-parallel manipulators are briefly reviewed and adopted for the forward and inverse displacement analysis for this mobile robot. Both loop-closure equations based on geometric constraints and the intersection of the loci of the feet are utilized to solve the forward displacement problem. Closed-form solutions are identified and discussed in the cases of redundant sensing with displacement information from nine, eight and seven joint angle sensors. For the non redundant sensing case using information from six joint angle sensors, it is shown that closed-form solutions can only be obtained when the displacement information is available from non-equally distributed joint angle sensors among the three legs. As for the case when joint angle sensors are equally distributed among the three legs, it will result in a 16th-order polynomial of a single variable. Finally, results from the simulations are presented for both inverse displacement analysis and the non redundant sensing case with equally distributed joint angle sensors. It was found that at most sixteen forward displacement solutions exist if displacement information from two joint angle sensors per leg are used and one is not used.

1. INTRODUCTION

The forward and inverse displacement analysis of an innovative three-legged mobile robot STriDER (Self-Excited Tripedal Dynamic Experimental Robot) that utilizes the concept of passive dynamic locomotion while walking is presented in this paper. STriDER can be modeled as a three-branch in-parallel manipulator given the assumption that all three feet are in contact with the ground with no slipping. Note that the methods used in the following analysis are only valid under this assumption and they are not valid when any of the feet leaves the ground or slips significantly. The stability margin of STriDER is described in [1] and the friction constraints of the feet are studied in [2,3]. [1-3] can be used to develop the criteria under which the assumptions above are valid.

In order to plan, observe and control the robot's posture changes, a forward and inverse displacement analysis must be completed. Forward and inverse displacement solutions are calculated by adopting kinematic analysis methods for in-parallel manipulators on STriDER. The forward displacement analysis for this mobile robot is solved by loop-closure

1. Address all correspondence to this author.

equations based on geometric constraints and the intersection of the loci of the feet. For redundant sensing with displacement information from nine, eight, and seven joint angle sensors, closed-form solutions are formed. For non redundant sensing cases, or displacement information from six joint angle sensors, closed-from solutions can be obtained when the displacement information is known from non-equally distributed joint angle sensors between the three legs. On the other hand, for equally distributed joint angle sensors, a 16th-order polynomial with one variable can be solved.

Section 2 presents the concept of STriDER, including; a novel tripedal gait, strategies for changing directions, kinematic configuration, and adaptation to a three-branch in-parallel manipulator. Section 3 first reviews and describes briefly the methodology of forward and inverse displacement analysis for in-parallel manipulators. These techniques are then adopted in Sections 3.1 and 3.2 to solve the inverse and forward displacement problems for STriDER. Section 4 includes numerical examples and results for both inverse and forward displacement simulations. Finally, Section 5 summarizes all concluded results and discusses future research.

2. BACKGROUND

The design and locomotion of robots are often inspired by nature; however, the three-legged walking machine presented here exemplifies an innovative tripedal gait. In this section, the kinematic configuration, link parameters, kinematic analysis for in-parallel manipulators are briefly reviewed and the connection between this mobile robot and three-branch in-parallel manipulators is explained.

2.1 STRIDER (SELF-EXCITED TRIPEDAL DYNAMIC EXPERIMENTAL ROBOT)

Unlike common bipeds, quadrupeds, and hexapods, STriDER (Self-excited Tripedal Dynamic Experimental Robot), shown in FIG. 1, is an innovative three-legged walking machine that incorporates the concept of actuated passive dynamic locomotion. This idea, introduced by Tad McGeer in the late 1980s, uses the natural built in dynamics of the robot to create the most efficient walking motion [4]. Furthermore, the proper mechanical design of a robot can provide energy efficient locomotion without sophisticated control methods [5,6]. However, STriDER is inherently stable with its tripod stance and can easily change directions.

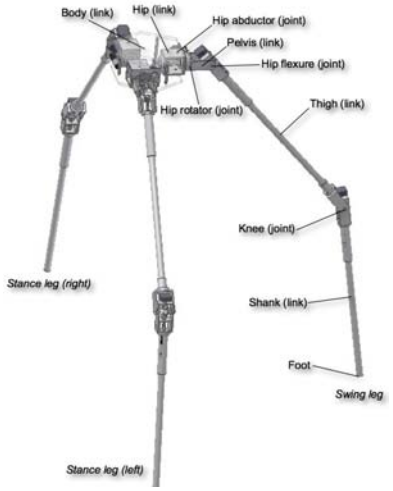

FIG. 1. STriDER (SELF-EXCITED TRIPEDAL DYNAMIC EXPERIMENTAL ROBOT)

The novel tripedal gait (patent pending) is simply implemented, as shown in FIG. 2 for a single step; a video is presented in [7]. During a step, two legs act as stance legs while the other acts as a swing leg. STriDER begins with a stable tripod stance (FIG. 2(a)), then the hip links are oriented to push the center of gravity forward by aligning the stance legs' pelvis links (FIG. 2(b)). As the body of the robot falls forward (FIG. 2(c)), the swing leg naturally swings in between the two stance legs (FIG. 2(d)) and catches the fall (FIG. 2(e)). As the robot takes a step, the body need to rotate 180° to prevent the legs from tangling up. Once all three legs are in contact with the ground, the robot regains its stability and the posture of the robot is reset in preparation for the next step (FIG. 2(f)) [8, 16, 17].

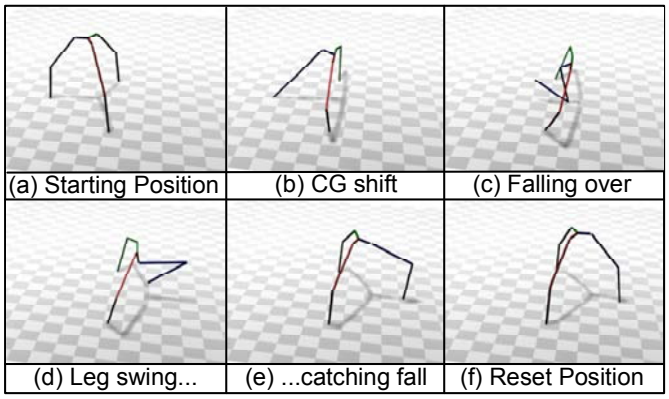

FIG. 2. SINGLE STEP TRIPEDAL GAIT

Gaits for changing directions can be implemented in a rather interesting way as illustrated in FIG. 3. By changing the sequence of choice of the swing leg, the tripedal gait can move the robot in 60° interval directions for each step [9].

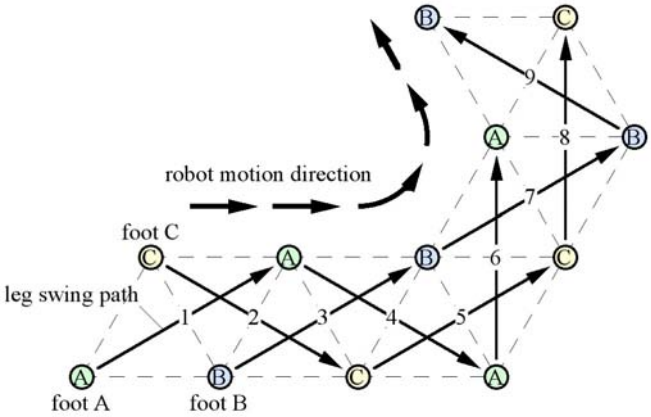

FIG. 3. GAIT FOR CHANGING DIRECTIONS

STriDER is developed for deploying sensors rather than for manipulation tasks. The tall nature of STriDER makes it ideal for surveillance since sensors such as cameras can be set at high positions. Two working prototypes of STriDER have been fabricated, as shown in FIG. 4. These models will be used in future experiments to examine STriDER's transitions between gaits, adaptation to various terrains, and stability analysis.

FIG. 4. STriDER PROTYPES

2.2 KINEMATIC CONFIGURATION OF STriDER

The definition of coordinate systems for each leg is shown in FIG. 5. The configuration for all three legs of STriDER is the same, thus the analysis for one leg is presented here as the other two legs will follow the same procedure. The subscript i denotes the leg number (i.e. i=1, 2, 3) in the coordinate frames, links, and joint labels.

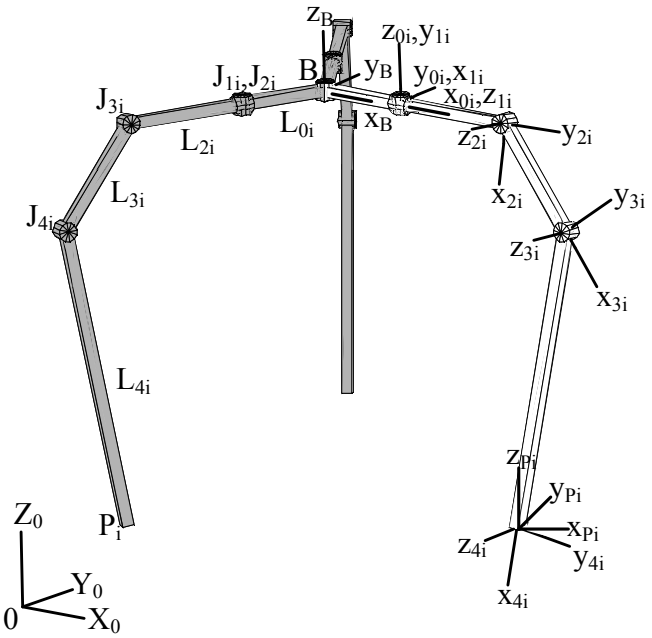

FIG. 5. COORDINATE FRAME AND JOINT DEFINITIONS

Table 1 lists the nomenclature used to define the coordinate frames, joint and links. First, a global coordinate system, $\{X_0, Y_0, Z_0\}$, is established and used as the reference for positions and orientations. Next, the body coordinate frame $\{x_B, y_B, z_B\}$ is defined as shown in FIG. 5. Each leg is separated by 120 degrees, leg one, leg two and leg three are 0 degrees, 120 degrees, and 240 degrees from the positive x_B axis, respectively. Each leg includes four actuated joints, J_{1i}, J_{2i}, J_{3i}, and J_{4i}. The hip abductor joint, J_{1i}, controls the stance leg's rotator joints to align during a step. In the first prototype of STriDER developed in [7], three independent abductor joints are used to accomplish the alignment. Later in [16], a new abductor joint mechanism to align the rotator joints driven by only one motor is used to replace the three motors abductors. Thus J_{1i} is not treated as an active joint in this paper. Next, J_{2i}, the hip rotator joint, allows the legs to rotate around the z_{1i} axis. J_{3i}, the hip flexure joint and $J_{4i,}$ the knee joint are both revolute joints that rotate around the z_{2i} and z_{3i} axes, respectively. Two coordinate frames $\{x_{4i}, y_{4i}, z_{4i}\}$ and $\{x_{Pi}, y_{Pi}, z_{Pi}\}$ are established at each foot. The three unit vectors in frame of $\{x_{Pi}, y_{Pi}, z_{Pi}\}$ are defined to be parallel to the global vector units. The foot contact points denoted by P_i are treated as spherical joints during analysis and $\{x_{4i}, y_{4i}, z_{4i}\}$ relates to $\{x_{Pi}, y_{Pi}, z_{Pi}\}$ with three Euler angles. Finally, the links listed as L_{0i}, L_{1i}, L_{2i}, L_{3i}, and L_{4i} are clearly labeled in FIG. 5 and represent the body link, hip link which is equal to zero, pelvis link, thigh link and shank link. Furthermore, links L_{01}, L_{02}, and L_{03} are constant values that form the body triangle.

TABLE 1. NOMENCLATURE

Nomenclature	
i:	Leg number (i=1,2,3)
$\{X_0, Y_0, Z_0\}$:	Global fixed coordinate system
$\{x_B, y_B, z_B\}$:	Body center coordinate system
J_{1i}:	Hip abductor joint for leg i
J_{2i}:	Hip rotator joint for leg i
J_{3i}:	Hip flexure joint for leg i
J_{4i}:	Knee joint for leg i
P_i:	Foot contact point for leg i
L_{0i}:	Body link for leg i
L_{1i}:	Hip link for leg i (length =0)
L_{2i}:	Pelvis link for leg i
L_{3i}:	Thigh link for leg i
L_{4i}:	Shank link for leg i

The coordinate systems are defined following the standard Denavit-Hartenberg's convention [10] and the link parameters are listed in Table 2 where, j is the link number, (j = 1,2,3,4), i is the leg number (i=1, 2, 3), a_{ji} equals the distance along x_{ji} from J_{ji} to the intersection of the x_{ji} and $z_{(j-1)i}$ axes, d_{ji} is the distance along $z_{(j-1)i}$ from $J_{(j-1)i}$ to the intersection of the x_{ji} and $z_{(j-1)i}$ axes, α_{ji} is the angle between $z_{(j-1)i}$ and z_{ji} measured about x_{ji}, and Θ_{ji} is the angle between the $x_{(j-1)i}$ and x_{ji} measured about $z_{(j-1)i}$. Also, when all Θ_{ji} are equal to zero, the legs form a right angle between L_{2i} and L_{3i}.

TABLE 2. LINK PARAMETERS

Link	a_{ji}	α_{ji}	d_{ji}	Θ_{ji}
1	$L_{1i}=0$	90°	0	$\Theta_{1i}+90°$
2	0	0	L_{2i}	$\Theta_{2i}-90°$
3	L_{3i}	0	0	Θ_{3i}
4	L_{4i}	0	0	Θ_{4i}

2.3 PARALLEL MANIPULATORS

STriDER can be considered as a three-branch in-parallel manipulator given the assumption that all three foot contact points are fixed on the ground, as shown in FIG.6. The ground is modeled as "the base" of a parallel manipulator, with the body as "the moving platform". Since the position of the foot doesn't change and the link can rotate around the contact point freely, the foot can be treated as a spherical joint connecting each leg to the ground. Given the fact that the knee joints, hip flexure joints and hip rotator joints are all revolute joints and each of the three legs mainly has two segments i.e. thigh and shank link, STriDER belongs to the class of in-parallel manipulators with kinematically simple branches proposed by Podhorodeski in 1994[11]. Since the foot joint is treated as a passive spherical joint with three degrees of freedom, each leg has a total of six degrees of freedom including both actuated and passive joints (3 d.o.f for the foot contact point, 1 d.o.f for the knee, flexure, rotator, respectively), thus allowing the body of STriDER to have full six degrees of freedom. The possible kinematic configurations of 6-d.o.f. three-branch in-parallel manipulators are enumerated by Ben-Horin[12]. According to his classifications based on joint types, STriDER is an example of 3-SRRR (Spherical-Revolute-Revolute-Revolute) manipulators.

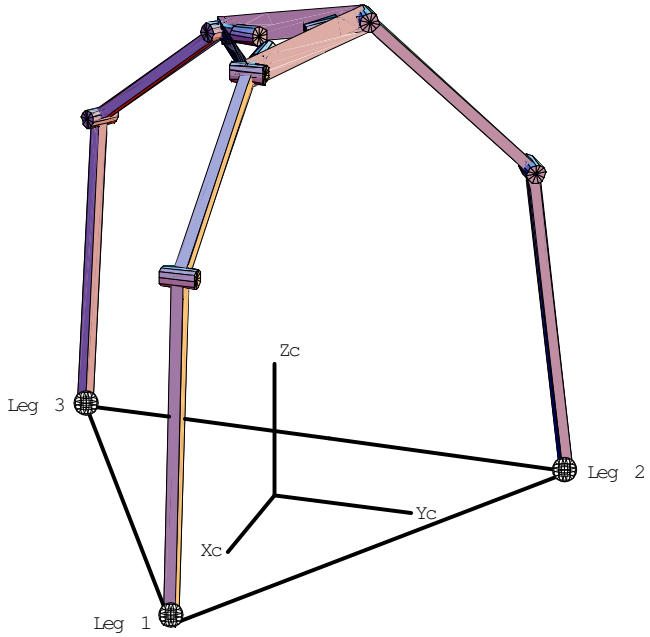

FIG. 6. GENERAL CASE REPRESENATION

When STriDER changes its position and orientation of its body without moving the feet of the legs, the characteristics of its motion can be analyzed with the well-established kinematics theory of three-branch in-parallel manipulators. However, because the feet are not really constrained to the ground, the stability region of STriDER is limited and the ground cannot generated reaction forces in any direction, which results in STriDER's smaller workspace than conventional parallel manipulators. A lot of research has been done on the forward and inverse kinematics of three-branch in-parallel manipulators. Innocenti and Parenti-Castelli[13] developed non-redundant direct position analysis on a Stewart platform mechanism with three branches. Notash and Podhorodeski[14] examined all the other redundant cases and came up with the complete forward displacement solutions for a class of three-branch parallel manipulators with only revolute joints. Later on, he furthered his work to include both revolute and prismatic joints [15]. The methodology used in the research mentioned above can be adopted to solve STriDER's inverse and forward displacement problem under its particularly new configuration of 3-SRRR. Rather than addressing the absolute position and orientation of the body in global coordinates, the paper focuses on the relative position and orientation between the body and the base.

3. INVERSE AND FORWARD DISPLACEMENT ANALYSIS

Unlike conventional robot arms or bipedal robots, the three-legs of STriDER with its main body form a three-branched parallel mechanism with changing posture. It is essential to thoroughly comprehend the inverse and forward displacement analysis in order to develop future strategies for dynamics, controls, path planning and changing directions, as well as, motion planning algorithms for generating stable tripedal gaits over uneven terrain. A full three-dimensional kinematic model was developed to aid in the inverse and forward displacement analysis process using *Mathematica*. This model will help examine the transitions between each gait. Also, the graphical simulation developed is beneficial for visualizing the motion of STriDER's links and joints.

3.1 INVERSE DISPLACEMENT ANALYSIS

The inverse displacement analysis is important for calculating the unknown internal angles Θ_{2i}, Θ_{3i}, and Θ_{4i} for the hip rotator, hip flexure and knee joints, respectively. As previously mentioned, the angle between the positive x_B axis and leg one, leg two and leg three is 0 degrees, 120 degrees, and 240 degrees, respectively. The angle between x_{0i} and x_{1i} measured about z_{0i}, Θ_{1i}, is set equal to zero and treated as a constant in these calculations. Also, the orientation and position of the body in relation to the global coordinate are known. So, the unknown angles Θ_{2i}, Θ_{3i}, and Θ_{4i} are calculated from the global body position and orientation, the angle between x_B and each leg, Θ_{1i}, and global foot positions. By treating the system as an elbow manipulator, as shown in FIG. 7, the unknown joint angle values can be determined. Note, in this figure, the leg is rotated 90 degrees around the x_{1i} axis for the ease of viewing.

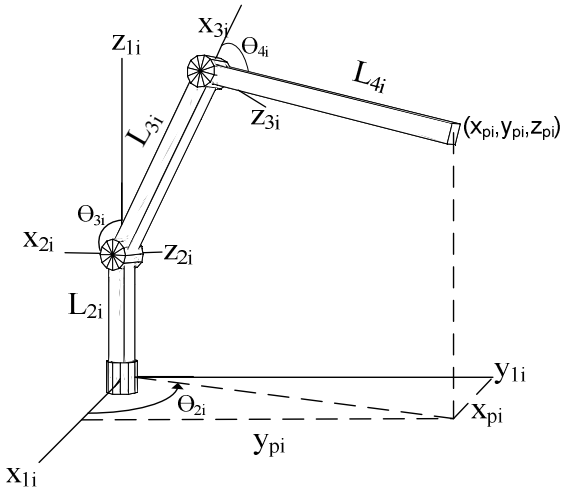

FIG. 7. ELBOW MANIPULATOR REPRESENTATION

Following the coordinate systems in FIG. 5, a homogeneous transformation from the global coordinate to the hip rotator joint was derived, as shown in Equation (1),

$$\mathbf{H}_o^{1i} = \mathbf{H}_o^B \mathbf{H}_B^{0i} \mathbf{H}_{0i}^{1i} = \begin{bmatrix} \mathbf{R}_o^{1i} & \mathbf{d}_o^{1i} \\ 0 & 1 \end{bmatrix}_{4x4} \tag{1}$$

where $\mathbf{R}_o^{1i}$ and $\mathbf{d}_o^{1i}$ specify the orientation and translation of $O_{x1i,y1i,z1i}$ relative to $O_{X0,Y0,Z0}$ respectively. Next, the orientation and translation of $O_{X0,Y0,Z0}$ relative to $O_{x1i,y1i,z1i}$ were found using Equations (2) and (3),

$$\mathbf{R}_{1i}^o = \left[\mathbf{R}_o^{1i}\right]^T \tag{2}$$

$$\mathbf{d}_{1i}^o = -\mathbf{R}_{1i}^o \mathbf{d}_o^{1i} \tag{3}$$

The orientation matrix, $\mathbf{R}_{1i}^o$, and translation vector, $\mathbf{d}_{1i}^o$, are used to find the translational vector, $\mathbf{d}_{1i}^{Pi}$, to relate the position of $O_{xPi,yPi,zPi}$ to $O_{x1i,y1i,z1i}$, as shown in Equation (4),

$$\mathbf{d}_{1i}^{Pi} = \mathbf{R}_{1i}^o \mathbf{d}_o^{Pi} + \mathbf{d}_{1i}^o = \begin{bmatrix} x_{Pi} \\ y_{Pi} \\ z_{Pi} \end{bmatrix} \tag{4}$$

where $\mathbf{d}_o^{Pi}$ is the foot position in relation to the global coordinates and vector $\begin{bmatrix} x_{Pi} & y_{Pi} & z_{Pi} \end{bmatrix}^T$ represents the foot position relative to the local hip rotator coordinates, which is also the base of the elbow manipulator shown in FIG. 7. This now becomes a common elbow manipulator problem [10].

The angle at the hip flexure joint, Θ_{2i}, is found using Equation (5),

$$\theta_{2i} = \text{Arctan}\,2\left(x_{Pi}, y_{Pi}\right) + \frac{\pi}{2} \tag{5}$$

where x_{Pi} and y_{Pi} are the x and y foot positions relative to the elbow manipulator base. Notice that 90 degrees are added to this value due to the link parameter definition listed in Table 2. Next, the angle at the knee joint, Θ_{4i}, is calculated, as shown in Equation (6),

$$\theta_{4i} = \text{Arctan}2\left(D, \pm\sqrt{1-D^2}\right) \tag{6}$$

where D is a constant term determined from Equation (7),

$$D = \frac{x_{Pi}^{\,2} + y_{Pi}^{\,2} + \left(z_{Pi} - L_{2i}\right)^2 - L_{3i}^{\,2} - L_{4i}^{\,2}}{2L_{3i}L_{4i}} \tag{7}$$

where L_{2i}, L_{3i}, and L_{4i} are link lengths and z_{Pi} is the z foot position relative to the base. As shown, with ± in Equation (6) there will be two values for Θ_{4i}, each corresponds to an elbow up or elbow down case. Thus, there will also be two corresponding values for Θ_{3i}, as calculated in Equation (8),

$$\theta_{3i} = \text{Arctan2}(\sqrt{x_{Pi}{}^2 + y_{Pi}{}^2}, z_{Pi} - L_{2i}) - \text{Arctan2}(L_{3i} + L_{4i}\cos\theta_{4i}, L_{4i}\sin\theta_{4i}) \quad (8)$$

In conclusion, if the body global position and orientation, the hip abductor joint angle Θ_{1i}, and the global foot positions are known, then the internal joint angles, hip rotator joint angle Θ_{2i}, hip flexure joint angle Θ_{3i}, and knee joint angle Θ_{4i} can be calculated by modeling the legs as elbow manipulators where the base is at the hip rotator joint and all link lengths are known and constant.

3.2 FORWARD DISPLAMENT ANALYSIS

The forward displacement solution requires resolving the position and orientation of the body with displacement information from the joint angle sensors. For the case of STriDER, it has a total of nine actuated joints. The nomenclature n_1 - n_2 – n_3 will be used to describe the sensing where n_i corresponds to the number of available displacement information from the joint angle sensors in leg i. For example, 3-2-1 means there are three sensed joint angles in leg 1, two sensed joint angles in leg 2 and 1 sensed joint angles in leg 3.

Since the body has 6 d.o.f, at least six joint angles out of nine are needed for feasible forward displacement solutions and each leg must have at least one known joint angle. All possible cases of joint sensing are listed as follows: (1)3-3-3 (nine joint angles sensed); (2) 3-3-2(eight joint angles sensed); (3) 3-3-1 and 3-2-2 (seven joint angles sensed); and (4) 3-2-1 and 2-2-2 (six joint angles sensed). Case 1, 2 and 3 are redundant sensing and case 4 is non-redundant sensing. Especially, in case 4, 3-2-1 is referred to non-equally distributed sensing and 2-2-2 is known as equally distributed sensing.

As a legged mobile robot, each joint of STriDER has to be both actuated and sensed in order to carry out versatile missions as mentioned in Section 2.1. However, under some particular conditions, certain sensors or actuators can be intentionally shut down as long as STriDER can handle. For example, during the swing phase of walking, some actuators on the swing leg are turned off in order to utilize the passive dynamic locomotion. Thus, forward displacement analysis on redundant and non-redundant sensing cases are both necessary. The fully sensed case of joint angles leads to a unique solution of the body position and orientation. If one or more joint angle sensor is broken, the information of the body can still be obtained by solving the forward displacement problems with less than 9 joint angles. The future research of STriDER, i.e. the singularity analysis, workspace analysis, etc., also needs the forward displacement analysis as an important tool.

3.2.1 NINE JOINT ANGLES SENSED CASE [3-3-3]

If all nine displacement information from the joint angle sensors is available, the location and orientation of the body has a unique solution. First assume the body is positioned at the global origin with zero orientation, and then with 3-3-3 sensing, the global position vector of each foot ${}^0\mathbf{P}_i$, i = 1,2,3, representing the leg number, can be calculated easily. These three contact points constitute a triangle in 3D space, which is treated as the imaginary "base" of the in-parallel manipulator. The location of the centroid of the base is described by:

$${}^0\mathbf{P}_c = ({}^0\mathbf{P}_1 + {}^0\mathbf{P}_2 + {}^0\mathbf{P}_3)/3 \quad (9)$$

Three orthogonal unit vectors describing the orientation of the base can be found as:

$$\begin{aligned} {}^0\mathbf{u}_x &= ({}^0\mathbf{P}_1 - {}^0\mathbf{P}_c)/\|(\mathbf{P}_1 - \mathbf{P}_c)\| \\ {}^0\mathbf{u}_z &= {}^0\mathbf{u}_x \times ({}^0\mathbf{P}_2 - {}^0\mathbf{P}_c)/\|(\mathbf{P}_2 - \mathbf{P}_c)\| \\ {}^0\mathbf{u}_y &= {}^0\mathbf{u}_z \times {}^0\mathbf{u}_x \end{aligned} \quad (10)$$

with ${}^0\mathbf{u}_z$ being the unit vector normal to the plane of the base, ${}^0\mathbf{u}_x$ being the unit vector pointing to the tip of leg 1, and ${}^0\mathbf{u}_y$ being the unit vector perpendicular to ${}^0\mathbf{u}_x$ and ${}^0\mathbf{u}_z$. The sign of $\|\ \|$ denotes the Euclidean norm. ${}^0\mathbf{u}_x$, ${}^0\mathbf{u}_y$, ${}^0\mathbf{u}_z$, together with the position vector ${}^0\mathbf{P}_c$ provide the homogenous transformation matrix $\mathbf{H}_0^B$ from the body frame B to the frame $\{x_c, y_c, z_c\}$ which locates at the centroid of the base triangle. Since the body is assumed at the origin with zero configuration, by taking the inverse of $\mathbf{H}_0^B$, the actual position and orientation of the body with respect to the global frame is derived.

Note that STriDER, as a mobile robot, doesn't have a real base with fixed geometry. If the robot only has joint sensors installed, the fully-sensed case with all sensors functional is the only way to get the geometry of the base. As long as the geometry of the base is known, the constraint equations of the foot position can be established. Then, fewer sensed joint angles can be used to derive the position and orientation of the body. This leads to the discussions of other sensing modes. The geometric relationships in the forward displacement problem of a three-branch in-parallel manipulator in redundant cases (eight or seven sensors) and the asymmetric non-redundant case (3-2-1) were discussed in [14], where Notash and Podhorodeski interpreted the feasible solutions as the intersections of different spatial shapes. Based on their method, the forward displacement solutions of STriDER in similar cases can be derived.

Generally, the calculation of the position and orientation of STriDER's body with less than 9 joint angles requires two steps. First assume the body is positioned at the global origin with zero orientation and solve the unsensed joint angles to obtain locations of the feet by using geometric constraints, either through looking for the intersections of various 3D shapes or through solving the loop-closure equations. Then use Equation (9) (10) and the inverse of $\mathbf{H}_0^B$ to derive the homogenous matrix which represents the body. Note that in the following sections, the geometric parameters of the base are assumed to be known and utilized to establish the constraints.

3.2.2 EIGHT JOINT ANGLES SENSED CASE [3-3-2]

Assume one sensor on leg 3 is broken or intentionally shut down. However, all the other joint sensors in leg 1 and 2 are still functional. The location of P_1 and P_2 can be expressed in terms of the known joint angles. As described in [11], with two points P_1 and P_2 fixed, the locus of the P_3 given the constraint of the base triangle becomes a spatial circle $C_{1,2}$ about the line passing through P_1 and P_2 with a radius MP_3. M is the projected point of P_3 on line P_1P_2. Meanwhile, with only one unknown joint angle in leg 3, the locus of P_3 under the constraint of leg 3 is also a spatial circle C_3 about certain joint axis.

As illustrated in FIG.8, $\boldsymbol{\theta}_4$ in leg 3 is assumed as the unsensed joint angle. Therefore two spatial circles $C_{1,2}$ and C_3 must intersect in at least one location in order to have a feasible solution. Once the location is determined, the position vector of P_3 is known. Using Equations (9) and (10) and taking the inverse of $\mathbf{H}_0^B$, the position and orientation of the body are determined. Note that the centers, radii and unit mutual orthogonal vectors of $C_{1,2}$ and C_3 respectively, can be found from known geometric parameters and sensed joint angles. $C_{1,2}$ and C_3 have at most two real intersections, which corresponds to two feasible forward displacement solutions. Since both $C_{1,2}$ and C_3 can be expressed as quadratic equations, closed-form solutions of the common roots can be derived.

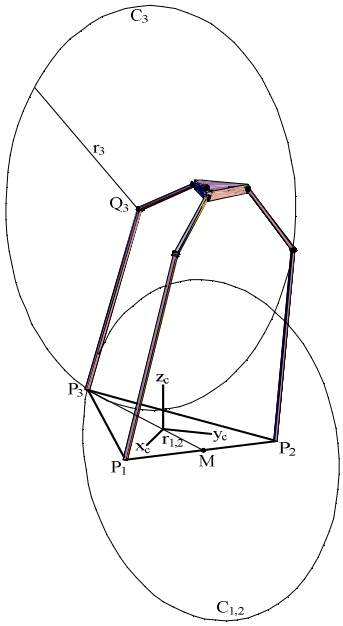

FIG.8. INTERSECTION OF TWO CIRCLES [3-3-2 CASE]

3.2.3 SEVEN JOINT ANGLES SENSED CASE [3-3-1 & 3-2-2]

3-3-1 Sensing

When the information of all six joint angles in leg 1 and leg2 is assumed to be available, the location of P_1 and P_2 can be expressed in terms of the sensed joint angles. Considering the constraint of the base triangle, the locus of P_3 is a spatial circle $C_{1,2}$ again. The locus of P_3 under the constraint of leg 3 will be a sphere, a torus, or a circular plane, depending on the relative position and directions of the unsensed joints [14]. The implementation of this method in STriDER is discussed in the following subsections for each of these three cases. Each intersection of the spatial shapes represents a feasible forward displacement solution.

Θ_{2i} & Θ_{3i} *unsensed*

Θ_2 and Θ_3 in leg 3 are assumed to be the unsensed joints, whose axes are intersecting with each other. The locus of the foot P_3 is the sphere S_3 as shown in FIG.9, with the center Q_3 locating at the intersecting point of axis z_{13} and z_{23}. The intersections of the sphere S_3 and the circle $C_{1,2}$ will be used to derive the forward displacement solutions. Generally, this case has up to two intersections.

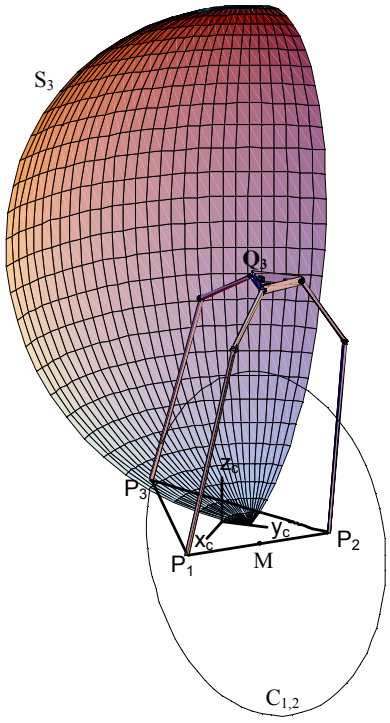

FIG. 9. SPHERE AND CIRCLE INTERSECTION [3-3-1 CASE]

Θ_{2i} & Θ_{4i} *unsensed*

Θ_2 and Θ_4 in leg 3 are assumed to be the unsensed joints. Since the axes of these two joints are skew axes and L_4 is longer than L_3, the locus of foot P_3 is the spindle torus T_3. A self-intersecting spindle torus is illustrated in FIG.10. It is a special type of torus when the length of the radius from the

center of the hole to the center of the torus is smaller than the length of the radius of the tube as described in [18]. As shown in FIG.11, the intersections of the torus T_3 and the circle $C_{1,2}$ will be used to derive the forward displacement solutions. There are a maximum of four intersections existing in this case.

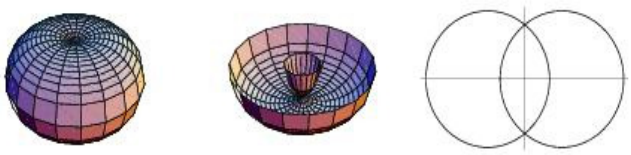

FIG. 10. SELF-INTERSECTION SPINDEL TORUS

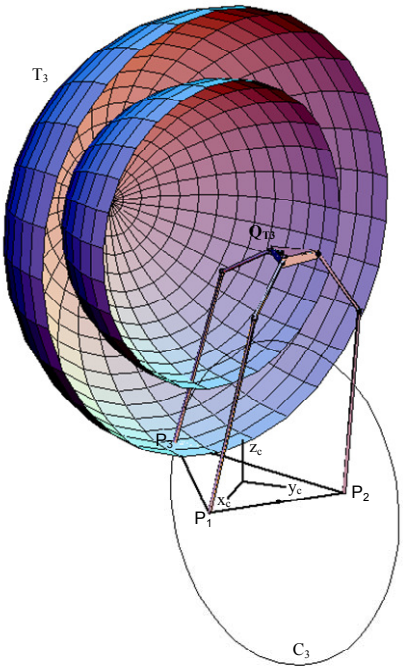

FIG. 11. TORUS AND CIRCLE INTERSECTION [3-3-1] CASE

Θ_{3i} & Θ_{4i} *unsensed*

Θ_3 and Θ_4 are assumed to be the unsensed joints in leg 3. Since their axes are parallel and L_4 is longer than L_3, the locus of foot P_3 is the circular plane CP_3 as shown in FIG.12. The intersections of the circular plane CP_3 and the circle $C_{1,2}$ will be used to derive the forward displacement solutions. There are up to two intersections of the circle $C_{1,2}$ and the circular plane CP_3

As a summary of the three cases discussed above, the geometric parameters of various spatial shapes (circle, sphere, torus, circular plane) are developed with known parameters and sensed joint angles. All of these shapes can be described with quadratic equations. The intersection points are determined through solving for the common roots of an equation representing the spatial circle and those 3D shapes (circle, sphere, torus, circular plane). Since the order of the polynomial systems are less or equal to four, closed-form solutions can be obtained. With each solution of the unsensed joint angle, the position vector P_3 is derived and the same procedures as the all joint angle sensed case [3-3-3] can be carried out to obtain the information of the body's position and orientation.

Mathematically, if a circle happens to be part of the sphere, the torus, or the circular plane, there exist infinity intersections which correspond to infinity forward displacement solutions. This is actually the singularity case in kinematic analysis, which will be fully discussed in future research.

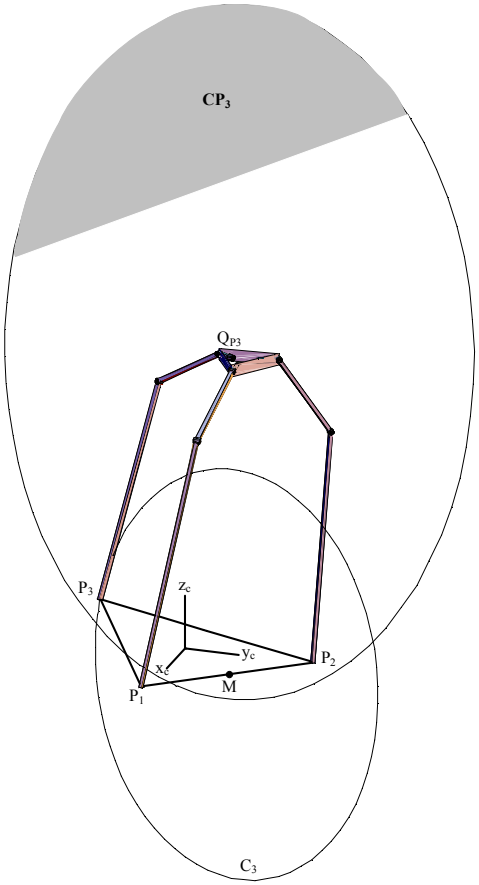

FIG.12. CIRCULAR PLANE AND CIRCLE INTERSECTION [3-3-1] CASE

3-2-2 Sensing

In the case of 3-2-2 sensing, the location of P_1 can be expressed with the sensed joint angles. For the leg with three sensed joint angles and any leg with two sensed joint angles, there exists a loop-closure constraint equation with respect to a single unsensed joint angle. For each of the solutions derived, the case of 3-2-2 sensing reduces to the 3-3-2 sensing and there are at most four solutions with closed-form as described in [14].

3.2.4. SIX JOINT ANGLES SENSED CASE [2-2-2 & 3-2-1]

2-2-2 Sensing

The 2-2-2 sensing case for STriDER is kinematically identical to the Stewart platform proposed by Innocenti and Parenti-Castelli in [13]. Three loop-closure equations are utilized to derive a 16^{th}-order polynomial with respect to a single variable. This indicates that at most 16 solutions may exist for 2-2-2 sensing. Since the order of the polynomial is much higher than four, only numerical solutions can be derived. Geometrically, the locus of each foot when two joint angles in each leg are sensed and one joint angle is not sensed is a spatial circle C_i (i = 1,2,3). These three equations will solve for the particular points on the circles that satisfy the geometric constraints of the base triangle $P_1P_2P_3$. A general example of this case is displayed in FIG.13.

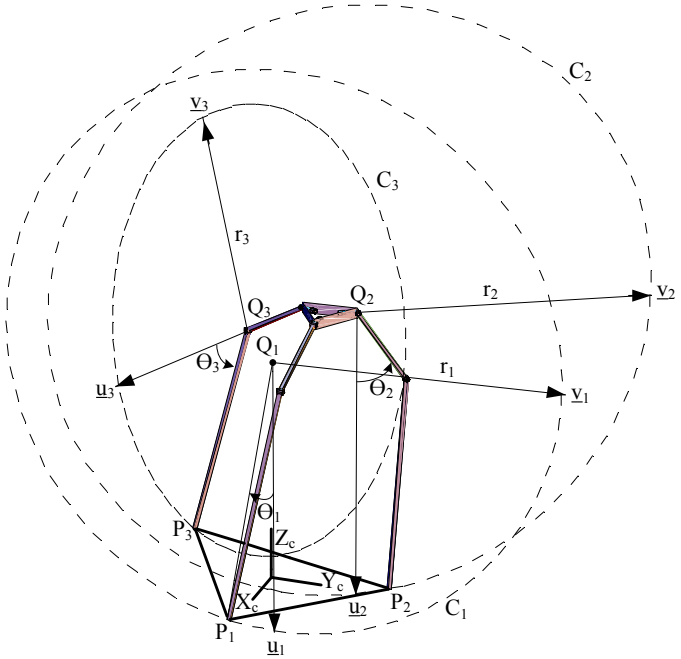

FIG.13. GENERAL NON REDUNDANT [2-2-2 CASE]

As shown in FIG.12, each leg has two sensed joint angles and one unsensed joint angle. The loci of P_1, P_2 and P_3 are three independent spatial circles C_1, C_2 and C_3 with the centers at Q_1, Q_2 and Q_3 respectively. For each loop $P_iP_{i+1}Q_{i+1}Q_i$, i = 1,2,3 (modulo3), the following vector equations can be written:

$$P_{i+1} - P_i = (P_{i+1} - Q_{i+1}) + (Q_{i+1} - Q_i) - (P_i - Q_i) \qquad (11)$$

$$\left|P_{i+1} - P_i\right| = d_{i(i+1)} \qquad (12)$$

$$P_i - Q_i = r_i\left(\mathbf{u_i}\cos\theta_i + \mathbf{v_i}\sin\theta_i\right) \qquad (13)$$

$$P_{i+1} - Q_{i+1} = r_{i+1}\left(\mathbf{u_{i+1}}\cos\theta_{i+1} + \mathbf{v_{i+1}}\sin\theta_{i+1}\right) \qquad (14)$$

where $\mathbf{u_i}$ and $\mathbf{v_i}$ are mutual orthogonal vector units parallel to the plane of the C_i circle, the direction of these two vector units are chosen such that the definitions of θ_i are consistent with Section 2.1; $d_{i(i+1)}$ represents the distance between P_i and P_{i+1}; r_i is the radius of C_i. Again, the information of $\mathbf{u_i}$, $\mathbf{v_i}$,Q_i ,r_i and $d_{i(i+1)}$ are uniquely defined by the know geometric parameters and sensed joint angles.

By squaring Equation (11), the following scalar equation is obtained:

$$\begin{aligned} &{}^iq_1C_iC_{i+1} + {}^iq_2C_iS_{i+1} + {}^iq_3S_iC_{i+1} + {}^iq_4S_iS_{i+1} + \\ &{}^iq_5C_i + {}^iq_6S_i + {}^iq_7C_{i+1} + {}^iq_8S_{i+1} + {}^iq_9 = 0 \end{aligned} \qquad (15)$$

where $C_i = \cos\theta_i$, $S_i = \sin\theta_i$, i = 1,2,3 (modulo3), and

$${}^iq_1 = 2\, r_i\, r_{i+1}\, \mathbf{u_i}\, \mathbf{u_{i+1}} \qquad (15.1)$$
$${}^iq_2 = 2\, r_i\, r_{i+1}\, \mathbf{u_i}\, \mathbf{v_{i+1}} \qquad (15.2)$$
$${}^iq_3 = 2\, r_i\, r_{i+1}\, \mathbf{v_i}\, \mathbf{u_{i+1}} \qquad (15.3)$$
$${}^iq_4 = 2\, r_i\, r_{i+1}\, \mathbf{v_i}\, \mathbf{u_{i+1}} \qquad (15.4)$$
$${}^iq_5 = 2\, r_i\, (Q_{i+1} - Q_i)\mathbf{u_i} \qquad (15.5)$$
$${}^iq_6 = 2\, r_i\, (Q_{i+1} - Q_i)\mathbf{v_i} \qquad (15.6)$$
$${}^iq_7 = 2\, r_{i+1}\, (Q_i - Q_{i+1})\mathbf{u_{i+1}} \qquad (15.7)$$
$${}^iq_8 = 2\, r_{i+1}\, (Q_i - Q_{i+1})\mathbf{v_{i+1}} \qquad (15.8)$$
$${}^iq_9 = d_{i(i+1)}{}^2 - r_i{}^2 - r_{(i+1)}{}^2 - (Q_{i+1}-Q_i)^2 \qquad (15.9)$$

Converting Equation (15) into a system of polynomial equations by substituting the trigonometric identities:

$$S_i = 2t_i/(1+t_i^2) \quad \text{and} \quad C_i = (1-t_i^2)/(1+t_i^2)$$

where $t_k = \tan(\theta_i/2)$, then Equation (15) can be written as follows:

$$\sum_{\substack{j=0,1,2\\k=0,1,2}} {}^ia_{jk}\, t_i^j\, t_{i+1}^k = 0 \qquad (16)$$

where i = 1,2,3 (modulo3)

$${}^ia_{00} = {}^iq_1 + {}^iq_5 + {}^iq_7 + {}^iq_9 \qquad (16.1)$$
$${}^ia_{01} = 2({}^iq_2 + {}^iq_8) \qquad (16.2)$$
$${}^ia_{02} = -{}^iq_1 + {}^iq_5 - {}^iq_7 + {}^iq_9 \qquad (16.3)$$
$${}^ia_{10} = 2({}^iq_3 + {}^iq_6) \qquad (16.4)$$
$${}^ia_{11} = 4\,{}^iq_4 \qquad (16.5)$$
$${}^ia_{12} = -2({}^iq_3 - {}^iq_6) \qquad (16.6)$$
$${}^ia_{20} = -{}^iq_1 - {}^iq_5 + {}^iq_7 + {}^iq_9 \qquad (16.7)$$
$${}^ia_{21} = -2({}^iq_2 - {}^iq_8) \qquad (16.8)$$
$${}^ia_{22} = {}^iq_1 - {}^iq_5 - {}^iq_7 + {}^iq_9 \qquad (16.9)$$

${}^iq_n$, n= 1-9 , are given in Equation (15.1)-(15.9)

The traditional 1-homogeneous Bezout number of Equation (16) is 4^3=64, however the 3-homogenous Bezout number is 16, which indicates this polynomial systems has 16 solutions. Using the Sylvester dialytic elimination method, Equation (16)

can be reduced to a 16^{th}-degree polynomial with respect to a single variable. Detailed procedures can be found in [13].

3-2-1 Sensing

In this case, there exists a loop-closure equation with 5 joint angles sensed and 1 joint angle unsensed. For each closed-form solution derived from this equation, the problem of locating P_3 reduces to the case of 3-3-1 sensing. The number of the solutions depends on the relative position and directions of the unsensed joints as discussed in Section 3.2.3. If two unsensed joint axes are intersecting or parallel, there are up to four forward displacement solutions. If two unsensed joint axes are skew, up to eight solutions may exist. All these solutions have closed-forms [14].

4. NUMERICAL EXAMPLES AND RESULTS

4.1 INVERSE DISPLACEMENT SIMULATION

The inverse displacement analysis displayed here relates to a general case. As mentioned in the inverse displacement analysis section, the known values for this calculation include; the global body position and orientation, Θ_{1i}, as well as all foot positions. Also the following link lengths were used, L_{0i}=0.0935 m, L_{1i}=0 m, L_{2i}=0.0935 m, L_{3i}=0.5 m, and L_{4i}=1.3 m. The base is assumed to be a equilateral triangle with the length of the side $d_{i(i+1)}$ = 1.24m.

Table 3 and Table 4 list the global body position and orientation and the global foot positions for each leg, respectively. The global frame $\{X_0, Y_0, Z_0\}$ is positioned at the centroid of the base for convenience. Once these values are selected, the step by step approach previously discussed in Section 3.1 is preformed.

TABLE 3. BODY POSITION AND ORIENTATION RELATIVE TO GLOBAL COORTINATES

X Rotation	10°
Y Rotation	5°
Z Rotation	0°
X Translation	0 m
Y Translation	0 m
Z Translation	1.6 m

TABLE 4. GLOBAL FOOT POSITIONS FOR EACH LEG

Foot Position	X (m)	Y (m)	Z (m)
P_1	0.716	0	0
P_2	-0.358	0.620	0
P_3	-0.358	-0.620	0

First, a homogenous transformation from the global coordinated to the hip rotator joint is preformed, as shown in Equation (1). Next, the relative location of each foot position to hip rotator joint is calculated using Equation (4). As previously stated, by treating each leg as an elbow manipulator the internal joint angles Θ_{2i}, Θ_{3i} and Θ_{4i} are calculated as shown in Equations (5), (6), and (8). Table 4 lists the results of these calculations for an elbow down scenario.

TABLE 5. INVERSE DISPLACEMENT ANALYSIS RESULTS (ELBOW DOWN)

Leg Number (i)	Θ_{2i}	Θ_{3i}	Θ_{4i}
1	-10°	59.628°	-49.243°
2	0.802°	34.781°	-38.275°
3	9.817°	61.252°	-49.877°

4.2 FORWARD DISPLACEMENT SIMULATION

With the data listed in Table 5, the forward displacement analysis in a 2-2-2 symmetric non-redundant sensing case is conducted. Without losing the generality, Θ_{21}, Θ_{32} and Θ_{43} are assumed to be the three unsensed joint angles and the rest joint angles are sensed. By carrying out the method in Section 3.2.4, 16 solutions are found and 6 among them are real solutions. These real solutions are verified by substituting back to Equation (16). The corresponding solutions of Θ_{ji} are listed in Table 6 and the postures of STriDER are plotted in FIG.14-FIG.19. All six postures only differ in the three unsensed joint angles. Among those solutons, solution 1, 2, 3 and 6 don't have a stable posture because the positions of the body are either below the ground or projected out of the range of base triangle. Solution 4 and 5 are stable with very subtle difference and note that solution 5 matches very well with the pre-specified joint angles.

TABLE 6. FORWARD DISPLACEMENT ANALYSIS RESULTS

Simulation number	Θ_{21}	Θ_{32}	Θ_{33}
1	174.937°	100.922°	138.802°
2	170.639°	190.845°	172.999°
3	-11.224°	34.111°	-132.854°
4	-6.965°	36.389°	-51.980°
5	-10°	34.781°	-49.877°
6	-10.416°	-38.078°	-49.597°

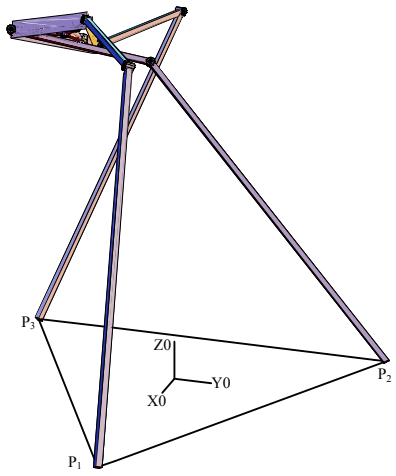

FIG.14. FORWARD DISPLACEMENT SOLUTION 1

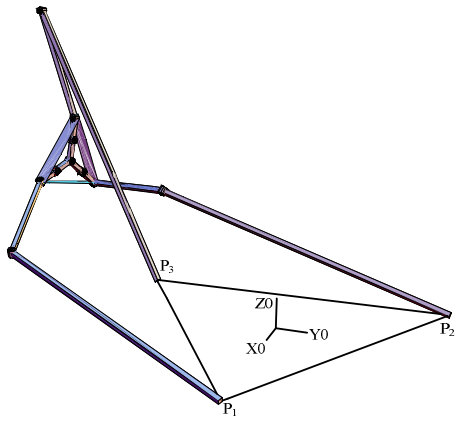

FIG.15. FORWARD DISPLACEMENT SOLUTION 2

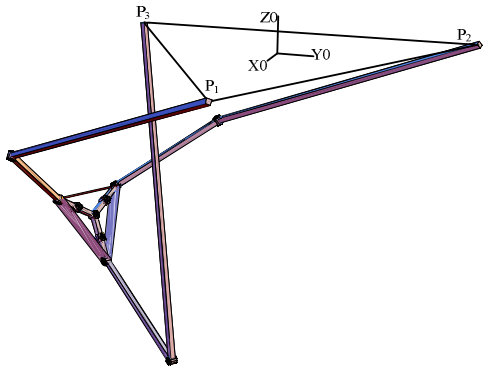

FIG.16. FORWARD DISPLACEMENT SOLUTION 3

5. CONCLUSION AND FUTURE RESEARCH

The inverse and forward displacement analysis of STriDER with all three feet fixed on the ground is discussed. The methods previously used to analyze the kinematics of three-branch manipulators, i.e. intersection of loci and close-loop equations, are adopted to solve the forward displacement problems on the particular case of STriDER. Results show that the forward displacement problem of multi-limbed mobile robots when all limbs are connected to the ground can be treated as the same kinematical problem of in-parallel manipulators.

Future research on the kinematics of STriDER will focus on the identification and elimination of the singular configurations, the Jacobian and workspace analysis and stable assembly modes. Since the feet of this robot are not actually fixed on the ground, the effects of slippery will also be investigated.

ACKNOWLEDGMENTS

The authors would like to thank the Office of Naval Research for their support for part of this work under Grant No. N00014-05-1-0828.

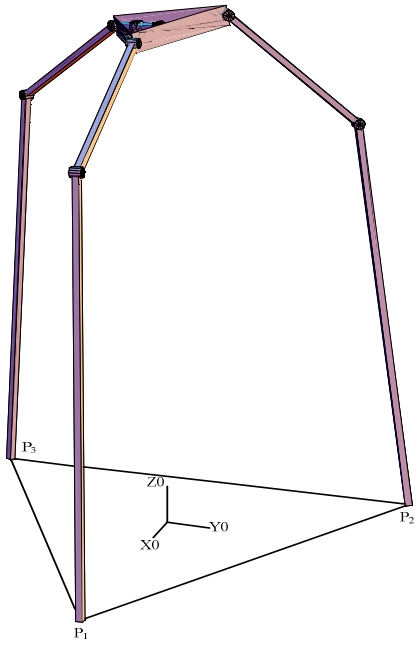

FIG.17. FORWARD DISPLACEMENT SOLUTION 4

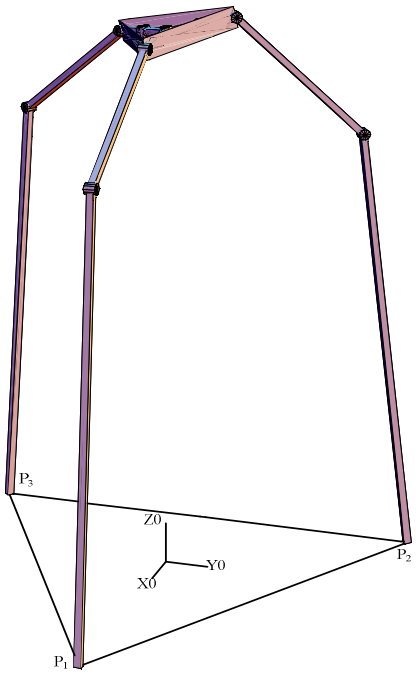

FIG.18. FORWARD DISPLACEMENT SOLUTION 5

FIG.19. FORWARD DISPLACEMENT SOLUTION 6

REFERENCES

[1] Morazzani, I., Lahr, D., Hong, D.W., Ren, P., "*Novel Tripedal Mobile Robot and Considerations for Gait Planning Strategies Based on Kinematics"* The 13th International Conference on Advanced Robotics, Jeju, Korea, August 21-14, 2007

[2] Hong, D. W., and Cipra, R. J., "*Visualization of the Contact Force Solution Space for Multi-Limbed Robots"* Journal of Mechanical Design, Vol.128, No.1, pp. 295–302, 2006

[3] Hong, D. W., and Cipra, R. J., "*Optimal Contact Force Distribution for Multi-Limbed Robots*" Journal of Mechanical Design, Vol.128, No.3, pp. 566-573, 2006

[4] McGeer, T., "*Passive dynamic walking*," Int. Journal of Robotics Research, Vol. 9, No. 2, pp. 62-82, April 1990.

[5] Tedrake, R., Zhang, T., Fong, M., Seung, H., "*Actuating a Simple 3D Passive Dynamic Walker*," IEEE International Conference, New Orleans, LA, April 2004, Vol. 5, pp. 4656-4661.

[6] Spong, M. W. and Bhatia, G., "*Further results on control of the compass gait biped,*" International Conference on Intelligent Robots and Systems, 2003, Las Vegas, Nevada, October 27-30, 2003, pp. 1933-1938.

[7] Heaston, J.R., Hong, D.W., Morazzani, I.M., Ren, P., Goldman, G., "*STriDER: Self-Excited Tripedal Dynamic Experimental Robot*", 2007 IEEE International Conference on Robotics and Automation, Roma, Italy, April 10-14.

[8] Heaston, J.R., "*Design of a Novel Tripedal Locomotion Robot and Simulation of a Dynamic Gait for a Single Step*", Masters Thesis, Virginia Polytechnic and State University, 2006.

[9] Hong, D.W., "*Biologically Inspired Locomotion Strategies: Novel Ground Mobile Robots at RoMeLa*", 2006 URAI International Conference on Ubiquitous Robots and Ambient Intelligence, Seoul, S. Korea, October 15-17, 2006.

[10] Spong, M.W, Vidyasagar, M., (1989) *Robot Dynamics and Control*, Canada: John Wiley & Sons, Inc.

[11] Podhorodeski, R.P, Pittens, K.H.,"*A Class of Parallel Manipulators based on Kinematically Simple Branches*," J. Mecha. Des., vol.116, pp. 908-914, 1994.

[12] Ben-Horin, P. and Shoham, M., "*Singularity Condition of Six-Degree-of-Freedom Three-Legged Parallel Robots Based on Grassmann-Cayley Algebra,*" IEEE Transactions on Robotics, Vol.22, No.4, August 2006

[13] Innocenti C. and Parenti-Castelli V., "*Direct Position Analysis of the Stewart Platform Mechanism*," Mech. Mach. Theory Vol.25, No.6. pp.611-621, 1990

[14]Notash L. and Podhorodeski R.P., "*Complete Forward Displacement Solutions for a Class of Three-Branch Parallel Manipulators*," Journal of Robotic Systems 11(96), 471-485 (1994)

[15] Notash L. and Podhorodeski R.P.,"*On the Forward Displacement Problem of Three-Branch Parallel Manipulators*," Mech. Mach. Theory Vol.30, No.3, pp.391 – 404, 1995

[16] Hong, D. W., and Lahr, D.F, "*Synthesis of the Body Swing Rotator Joint Aligning Mechanism for the Abductor Joint of a Novel Tripedal Locomotion Robot"*, 31st ASME Mechanisms and Robotics Conference, Las Vegas, Nevada, September 4-7, 2007.

[17] Heaston, J. and Hong, D. W., "*Design Optimization of a Novel Tripedal Locomotion Robot Through Simulation and Experiments for a Single Step Dynamic Gait*", 31st ASME Mechanisms and Robotics Conference, Las Vegas, Nevada, September 4-7, 2007.

[18] Pinkall, U. "Cyclides of Dupin." §3.3 in *Mathematical Models from the Collections of Universities and Museums* (Ed. G. Fischer). Braunschweig, Germany: Vieweg, pp. 28-30, 1986

